Hurricane intensification along U. S. coast suppressed during active hurricane periods

James P. Kossin[1]

[1]NOAA National Centers for Environmental Information, Center for Weather and Climate,
1225 W. Dayton St., Madison, WI 53706 USA (james.kossin@noaa.gov)

The North Atlantic ocean/atmosphere environment exhibits pronounced interdecadal variability that is known to strongly modulate Atlantic hurricane activity[1–6]. Sea surface temperature (SST) variability is correlated with hurricane variability through its relationship with the genesis and thermodynamic potential intensity of hurricanes[7]. Another critical factor governing hurricane genesis and intensity is ambient environmental vertical wind shear[8–10] (VWS). Warmer SST generally relates to more frequent genesis and greater potential intensity while VWS is a major factor that inhibits genesis and keeps hurricanes that do form from reaching their potential intensity. When averaged over the Atlantic hurricane main-development-region, SST and VWS co-vary inversely[11,12] so that the two factors act in concert to either enhance or inhibit basin-wide hurricane activity. Here I will show, however, that the regional patterns of variability are essential, and that conditions conducive to greater basin-wide hurricane activity occur systematically in tandem with conditions for more probable weakening of hurricanes near the United States (US) coast. In this case, the VWS and SST form a protective barrier along the US coast during periods of heightened basin-wide hurricane activity. Conversely, during the last period of quiescence, hurricanes [and particularly major (Category 3–5) hurricanes] near the US coast, while substantially less frequent, exhibited much greater intensification rate variance and were much more likely to rapidly intensify. This poses greater challenges to operational forecasting and, consequently, greater coastal risk during these hurricane events.

The annual frequency of Atlantic hurricanes, and particularly major (Category 3–5) hurricanes, exhibit coherent interdecadal variability (Fig. 1a,b). Hurricane seasons during the period from the late-1960s to mid-1990s were comparatively quiescent, and during periods prior and subsequent to this, seasonal hurricane activity was comparatively active. Hurricanes are known to be modulated by their ambient environmental conditions, particularly by sea surface temperature (SST) through its relationship with thermodynamic potential intensity[7], and vertical wind shear (VWS), which inhibits hurricanes from reaching or maintaining their potential intensity[8–10]. During the more active (quiescent) hurricane periods, SST in the hurricane main-development region (MDR) is anomalously warm (cool) and VWS is anomalously weak (strong) (Fig. 1c,d).

The interdecadal SST and VWS variability in the MDR, or simply the tropical North Atlantic, is well correlated to basin-wide hurricane activity, but does not provide an adequate picture when

considering intrabasin variability. In particular, the patterns of variability exhibit pronounced intrabasin differences between the MDR and regions closer to the US coast (Fig. 2). During periods of anomalously warm SST and weak VWS in the MDR, which coincide with enhanced basin-wide activity, the VWS along the US coast tends to be anomalously high while the SST anomalies in the region are substantially smaller than found in the MDR. Of particular relevance to hazard exposure and mortality risk is the relationship between basin-wide activity and US landfall activity[13–19]. Here the question of whether the patterns of variability seen in Fig. 2 project onto this relationship is addressed.

As discussed above, VWS inhibits hurricanes from reaching or maintaining their thermodynamic potential intensity. That is, VWS acts as an intensity braking mechanism and hurricanes that move into higher VWS are expected to weaken (or intensify more slowly). In this case then, the enhanced VWS during more active periods of hurricane activity is expected to weaken hurricanes that approach or move along the US coast. This signal becomes clear when hurricane intensification rates in the region where hurricanes near the US coast (denoted by the northernmost white-outlined region in Fig. 2) are separated by active and quiescent periods (Fig. 3 and Table 1). The mean intensification rates between the active and quiescent periods are well-separated for hurricanes, and particularly major hurricanes for which the mean rates are negative in both active periods and positive during the quiescent period (Table 1). The mean rates tend to be near zero, as steady state intensity is most likely, with the exception of major hurricanes during the quiescent period, which are most likely to intensify by 5 kt in any given 6-hour period (Fig. 3a–d). Although the differences in the mean are statistically significant (at 90% confidence or greater), they are fairly small. The more pronounced differences are found in the variances, as the intensification rate distributions for the quiescent period are less leptokurtic with distinctly broader tails. For major hurricanes near the US coast, the intensification rate variance is 2 times (3 times) greater during the quiescent period compared to the prior (subsequent) active periods. This elevated variance, or volatility, in intensification rates during quiescent periods, which is not just a manifestation of the smaller sample size (see Methods), would very likely introduce substantial additional forecasting and warning challenges as these hurricanes and major hurricanes approach or move along the US coast.

As tacitly expected, there are fewer basin-wide hurricanes during the period of quiescence and substantially fewer major hurricanes (Table 1), but when a hurricane or major hurricane is near the US coast, the probability of intensification is substantially greater during the period of basin-wide quiescence (Fig. 3 and Table 2). The probability that a hurricane near the US coast during the quiescent period would intensify by 10 kt or greater in the following 6 hours was roughly twice that of a hurricane near the coast during the active periods (Fig. 3e and Table 2). The probability of intensification by 15 kt or greater in 6 hours was 2 times (3 times) more likely during the quiescent period compared to the prior (subsequent) active period. For major hurricanes, the differences are larger. A major hurricane near the US coast during the quiescent

period was about 2 times (4 times) more likely to intensify by 10 kt or greater and 3 times (6 times) more likely to intensify by 15 kt or greater in the following 6 hours compared to the prior (subsequent) active period (Fig. 3f and Table 2). Rapid intensification near the coast poses a very significant risk because it is difficult to forecast and shortens public warning time[20,21].

In the hurricane MDR, anomalously warm SST occurs concurrently with anomalously weak VWS, and vice versa, so that the two factors operate in concert to either enhance or inhibit basin-wide hurricane activity[11,12]. This is not the case, however, when the region along and near the US coast is considered. In this region, during periods of anomalously warm MDR SST, VWS is anomalously strong and the local SST anomalies are substantially weaker. That is, the VWS and SST in this region tend to operate in concert to inhibit intensification during periods when the MDR is conducive to it. This region is where hurricanes approaching the US coast must track, and thus the environmental conditions act as a coastal barrier during periods when basin-wide activity is elevated. The shift of intensification rates of major hurricanes near the US coast between periods of active and quiescent hurricane seasons is particularly pronounced, and the probability that a major hurricane near the US coast will undergo rapid intensification was comparatively much higher during the last quiescent period.

The patterns of variability and co-variability of SST and VWS described here are congruent with the patterns forced by the Atlantic Meridional Mode (AMM)[11,12]. The AMM is the leading mode of coupled ocean–atmosphere variability in the Atlantic and operates on interannual to interdecadal timescales. The AMM can be described as an intrinsic dynamic mode that is established through a wind-evaporation-SST feedback process[12], which provides a plausible physical-dynamical foundation for understanding the relationship between MDR hurricane activity and suppression of intensification along the US coast. Further empirical and numerical modeling explorations of this potential linkage, particularly on interdecadal timescales, are warranted.

The results here raise questions regarding what may be expected if environmental conditions shift back toward the pattern of the previous quiescent period[22,23], as well as what may be expected as the tropics continue to warm. The VWS pattern shown in Fig. 2 exhibits marked interdecadal variability but no trend since 1948. However, there is a significant SST trend that projects onto the interdecadal variability, which can be seen by the trend in the leading principal component time series (blue line in Fig. 2c). The SST trend pattern (Fig. 4) shows significant increasing trends throughout the MDR, but essentially no trend along the US coast. Considering this in tandem with the pattern of VWS variability (Fig. 2a), the effects of interdecadal VWS variability on hurricanes near the US coast have not been strongly compounded or offset by SST variability or trends. That is, the amplitude of both the interdecadal variability and trend of SST have minima along the US coast (Figs. 2b & 4), and appear to be playing only a minor role in modulating conditions there. It is not clear that this behavior will remain stationary under

projected continued warming of the tropics, but there is a potential that future warming will not strongly affect the control of VWS on these hurricanes.

As a closing note, the inverse relationship between variability in the MDR and the region along the US coast may help to explain the weak relationship between US landfalling hurricane frequency and basin-wide frequency[13–19, 24] by tempering US landfall frequency increases during active periods. Similarly, the present "drought" of US major hurricane landfalls[25,26] could plausibly be explained, in part, by this relationship. Given the potential impacts on US coastal hazard risk, this relationship merits further observational and modeling study.

References

1. Gray, W.M., J.D. Sheaffer, and C.W. Landsea, 1997: Climate trends associated with multidecadal variability of Atlantic hurricane activity. "Hurricanes: Climate and Socioeconomic Impacts." H.F. Diaz and R.S. Pulwarty, Eds., Springer-Verlag, New York, pp. 15-53.
2. Goldenberg, S. B., Landsea, C. W., Mestas-Nuñez, A. M. & Gray, W. M. *Science* **293,** 474–479 (2001).
3. Mann, M. E., and K. A. Emanuel (2006), Atlantic hurricane trends linked to climate change, EOS Trans. AGU, 87, 233–244, doi:10.1029/2006EO240001.
4. Knutson, T. R., J. L. McBride, J. Chan, K. Emanuel, G. Holland, C. Landsea, I. Held, J. P. Kossin, A. K. Srivastava, and M. Sugi, 2010: Tropical cyclones and climate change. *Nature Geoscience*, **3**, doi:10.1038/ngeo779.
5. Bindoff, N. L., and Coauthors, 2014: Detection and attribution of climate change: from global to regional. *Climate Change 2013: The Physical Science Basis*, T. F. Stocker et al., Eds., Cambridge University Press, 867–952.
6. Walsh, K. J. E., J. L. McBride, P. J. Klotzbach, S. Balachandran, S. J. Camargo, G. Holland, T. R. Knutson, J. P. Kossin, T.-C. Lee, A. Sobel, and M. Sugi, 2016: Tropical cyclones and climate change. *WIREs Climate Change*, **7**, 65-89, doi:10.1002/wcc371.
7. Emanuel, K., 2008: The Hurricane-Climate Connection. Bull. Amer. Meteor. Soc., 89, ES10-ES20.
8. DeMaria, M. (1996), The effect of vertical shear on tropical cyclone intensity change, J. Atmos. Sci., 53, 2076–2088.
9. Elsberry, R. L., and R. A. Jeffries, 1996: Vertical wind shear influences on tropical cyclone formation and intensification during TCM-92 and TCM-93. Mon. Wea. Rev., 124, 1374–1387.
10. Wang, M. L. M., and J. C. L. Chan (2004), Tropical cyclone intensity in vertical wind shear, J. Atmos. Sci., 61, 1859–1876.
11. Vimont, D. J., and J. P. Kossin, 2007: The Atlantic meridional mode and hurricane activity. Geophys. Res. Lett., 34, L07709, DOI:10.1029/2007GL029683.
12. Kossin, J. P., and D. J. Vimont, 2007: A more general framework for understanding Atlantic hurricane variability and trends. Bull. Amer. Meteor. Soc., 88, 1767-1781.
13. Holland, G. J., 2007: Misuse of landfall as a proxy for Atlantic tropical cyclone activity. Eos, Trans. Amer. Geophys. Union, 88, 349–356, doi:10.1029/2007EO360001.

14. Coughlin, K., E. Bellone, T. Leapple, S. Jewson, and K. Nzerem, 2009: A relationship between all Atlantic hurricanes and those that make landfall in the USA. Quart. J. Roy. Meteor. Soc., 135, 371–379.
15. Dailey, P. S., G. Zuba, G. Ljung, I. M. Dima, and J. Guin, 2009: On the relationship between North Atlantic sea surface temperatures and U.S. hurricane landfall risk. J. Appl. Meteor. Climatol., 48, 111–129.
16. Vecchi, G. A., and T. R. Knutson, 2011: Estimating annual numbers of Atlantic hurricanes missing from the HURDAT database (1878–1965) using ship track density. J. Climate, 24, 1736–1746, doi:10.1175/2010JCLI3810.1.
17. Villarini, G., G.A. Vecchi, and J.A. Smith, U.S. landfalling and North Atlantic hurricanes: Statistical modeling of their frequencies and ratios, Monthly Weather Review, 140(1), 44-65, 2012.
18. Landsea, C. W., 2015: Comments on "Monitoring and understanding trends in extreme storms: State of knowledge." Bull. Amer. Meteor. Soc., 96, 1175–1176, doi:10.1175/JCLI-D-13-00211.1.
19. Kossin, J. P., T. R. Karl, T. R. Knutson, K. A. Emanuel, K. E. Kunkel, and J. J. O'Brien, 2015: Reply to 'Comment on "Monitoring and Understanding Trends in Extreme Storms - State of Knowledge"' *Bull. Amer. Meteor. Soc.*, **96**, 1177–1179.
20. Kaplan, J., C. M. Rozoff, M. DeMaria, C. R. Sampson, J. P. Kossin, C. S. Velden, J. J. Cione, J. P. Dunion, J. A. Knaff, J. A. Zhang, J. F. Dostalek, J. D. Hawkins, T. F. Lee, and J. E. Solbrig, 2016: Evaluating environmental impacts on tropical cyclone rapid intensification predictability utilizing statistical models. *Wea. Forecasting*, **30**, 1374-1396.
21. Emanuel, K., 2016: Will Global Warming Make Hurricane Forecasting More Difficult? *Bull. Amer. Meteor. Soc.*, in press.
22. McCarthy G. D., Haigh, I. D., Hirschi, J.-M., Grist, J. P. & Smeed, D. A. *Nature* **521,** 508–510 (2015).
23. Klotzbach, P., Gray, W., & Fogarty, C. *Nature Geosci*. **8**, 737–738 (2015).
24. Emanuel, K., 2011: Global warming effects on U.S. hurricane damage. Wea. Climate Soc., 3, 261–268, doi:10.1175/WCAS-D-11-00007.1.
25. Hall, T. M., and K. Heried, 2015: The frequency and duration of U.S. hurricane droughts, Geophys. Res. Lett., 42, do:10.1002/2015GL063652.
26. Hart, R., D. Chavas, and M. Guishard 2015: The arbitrary definition of the current Atlantic major hurricane landfall drought. Bull. Amer. Meteor. Soc., 97, 713–722.
27. Landsea, C. W., and J. L. Franklin, 2013: Atlantic Hurricane Database Uncertainty and Presentation of a New Database Format. Mon. Wea. Rev., 141, 3576-3592
28. Kossin, J. P., T. L. Olander, and K. R. Knapp, 2013: Trend analysis with a new global record of tropical cyclone intensity. *J. Climate*, **26**, 9960-9976.
29. Kalnay et al.,The NCEP/NCAR 40-year reanalysis project, Bull. Amer. Meteor. Soc., 77, 437-470, 1996.
30. Huang, B., V.F. Banzon, E. Freeman, J. Lawrimore, W. Liu, T.C. Peterson, T.M. Smith, P.W. Thorne, S.D. Woodruff, and H.-M. Zhang, 2014: Extended Reconstructed Sea Surface Temperature version 4 (ERSST.v4): Part I. Upgrades and intercomparisons. Journal of Climate, in press, doi:10.1175/JCLI-D-14-00006.1

Acknowledgements
NOAA_ERSST_V4 and NCEP Reanalysis data were provided by the NOAA/OAR/ESRL PSD, Boulder, Colorado, USA, from their Web site at http://www.esrl.noaa.gov/psd/. HURDAT2 data are provided by the U. S. National Hurricane Center at their Web site http://www.nhc.noaa.gov/data/. The original manuscript benefitted greatly from the comments and suggestions of Michael White.

Author contributions
All analyses and writing were conducted by JPK.

The author declares no competing financial interests.

Methods

Hurricane data were taken from the HURDAT2 archive maintained by the U. S. National Hurricane Center, which provide 6-hourly "best-track fixes" with the location of the storm center and an estimate of the maximum wind-speed (intensity) for each storm[27]. Intensities are provided in 5 kt increments. The HURDAT2 file used here is "hurdat2-1851-2015-021716.txt" (see Data availability section below). The standard Saffir-Simpson scale was used to categorize the hurricanes. HURDAT2 data quality varies by time period considered[28]. Aircraft reconnaissance into hurricanes began in the 1940s, and meteorological satellite data became available in the late-1960s (polar orbiting satellites) to early-1970s (geostationary satellites). Here the data were separated into three 23-yr periods with the earliest period being post-reconnaissance but mostly pre-satellite, and are thus somewhat less reliable than the later data.

VWS was calculated from daily-mean winds from the NCEP/NCAR R1 reanalysis data[29]. The data begin in 1948 and are provided in units of m s^{-1}. For each day, the zonal and meridional wind components were used to form the wind vectors at low level (pressure level 850 hPa) and upper level (200 hPa). The magnitude of the vector difference between the 200 hPa and 850 hPa winds provides the mean daily shear, which was then used to compute monthly averages (see Code availability section below). The SST is based on monthly mean data from NOAA Extended Reconstructed Sea Surface Temperature V4 (ref. 30). The VWS and SST were averaged over the main hurricane season (Aug–Oct) and standardized at each location using the local mean and standard deviation, which were calculated from the full 68-year time series (1948–2015) at each location. Principal component analysis (PCA) was applied to the standardized data. The data are gridded and were weighted by latitude prior to PCA. The VWS and SST loading patterns shown in Fig. 2 were formed by regressing the first principal component of each onto the un-weighted standardized data. The leading loading patterns explain 20% and 56% of the variance of VWS and SST, respectively, and their eigenvalues are well-separated from those of the second loading patterns.

Probability density functions of intensity change were formed using the intensity difference between successive 6-hourly fixes for all cases within the northern region outlined in Fig. 2a (22.5°– 40°N and 262°– 297.5°E) and for each 23-yr period. The first of the two successive fixes had to have at least hurricane intensity (Fig. 3a) or major hurricane intensity (Fig. 3b) and both fixes were always required to be over water (to avoid capturing weakening due to landfall). Error bars in Fig. 3a,b were computed using bootstrap sampling. The error bars span two standard errors from the bootstrapped means of each 5 kt bin.

Empirical cumulative distribution functions (Fig. 3c,d) were computed using the Kaplan-Meier estimator, and the confidence bounds were determined using Greenwood's formula. Statistical significance of the separation of the means in Table 1 was determined with a Student's t-test, and the significance of the separation of the variance was based on a standard F-test. As a robustness

test for the separation of variance, the samples during the active periods were randomly subsampled 100,000 times, with replacement, to the smaller size of the quiescent period sample (Table 1). For both hurricanes and major hurricanes, the variance of the quiescent period sample is larger than the 99th percentile of variances from the random subsamples of the active periods (see Code availability section below).

The trend map of SST shown in Fig. 4 is based on standardized data as described above. Statistical significance of the trend at each location was determined with degrees of freedom adjusted as necessary for autocorrelation. The degrees of freedom were adjusted if the 68-yr time series at that location failed a Durbin-Watson test, which was applied to the residuals of the regression of SST onto year.

Code availability

The Code used to analyze the data and create the graphics are available at the GitHub repository: https://github.com/jpkossin/Nature_code_data/upload/master

Data availability

HURDAT2 data are available at http://www.nhc.noaa.gov/data/#hurdat. Note that these data are periodically reanalyzed and updated to a new version. The version used here is available via the GitHub repository.

The high-resolution bathymetry data used to create a landflag are available at: https://www.ngdc.noaa.gov/mgg/global/relief/ETOPO2/ETOPO2v2-2006/ETOPO2v2g/ NOAA_ERSST_V4 and NCEP Reanalysis data were provided by the NOAA/OAR/ESRL PSD, Boulder, Colorado, USA, from their Web site at http://www.esrl.noaa.gov/psd/.

Tables (and table legends)

Table 1 | Means and variances of 6-hr intensification rates near the US coast. Values show the mean rates [in units of ΔV (kt) per 6-hours] and the intensification rate variance for hurricanes (HU) and major hurricanes (MH) near the US coast (within the northernmost white-outlined region of Fig. 2a, but only over water) in each of the 23-year periods. Sample size is also shown along with the counts of basin-wide hurricanes and major hurricanes and the number of storms that were hurricanes and major hurricanes while near the US coast. Statistically significant separation of the means and variances of each active period compared to the quiescent period are denoted by the asterisks (*, **, *** denote 90%, 95%, 99% confidence, respectively).

	Mean		Variance		Sample Size		Basin-Wide Count		Near-Coast Count	
	HU	MH	HU	MH	HU	MH	HU	MH	HU	MH
1947–1969	+0.6**	–0.5*	32.3***	32.8***	1077	313	149	68	101	48
1970–1992	+1.4	+0.9	53.3	103.7	429	79	119	37	65	23
1993–2015	–0.2***	–1.5**	40.5***	55.5***	735	197	165	72	88	35

Table 2 | Probabilities of exceedance of 6-hr intensification rates near the US coast. Values show the probabilities (and their 95% confidence intervals) that the 6-hr intensity change was equal to or exceeded 5, 10, and 15 kt for hurricanes (HU) and major hurricanes (MH) near the US coast in each of the 23-year periods.

	Pr (ΔV ≥ 5 kt)		Pr (ΔV ≥ 10 kt)		Pr (ΔV ≥ 15 kt)	
	HU	MH	HU	MH	HU	MH
1947–1969	0.310±0.028	0.230±0.047	0.079±0.016	0.061±0.027	0.022±0.009	0.016±0.014
1970–1992	0.429±0.047	0.468±0.110	0.147±0.034	0.228±0.093	0.058±0.022	0.101±0.067
1993–2015	0.263±0.032	0.239±0.060	0.086±0.020	0.096±0.041	0.033±0.013	0.031±0.024

Figure legends

Figure 1 | Interdecadal variability of basin-wide Atlantic hurricane frequency and MDR environmental conditions. Time series of detrended annual basin-wide frequency of hurricanes (**a**) and major hurricanes (**b**), and main development region VWS (**c**) and SST (**d**). VWS and SST are shown in units of m s^{-1} and °C respectively. Thick black lines show time series smoothed with a 11-yr centered mean filter. The MDR is defined here as the region 10°–20°N and 275°–340°E.

Figure 2 | Patterns of Atlantic VWS and SST variability. Leading Principal Component Analysis loading patterns of VWS (**a**) and SST (**b**), and their associated principal component time series (**c**). The white-outlined regions in (**a**) are the hurricane MDR (tropical N. Atlantic) and the region that hurricanes approaching the US coast track through. The loading patterns have units of local standard deviation from local mean.

Figure 3 | Probability distributions of observed intensification rates near the US coast. Probability density distributions of 6-hr intensity change for hurricanes (**a**) and major hurricanes (**b**) during comparatively active (1947–1969 and 1993–2015) and quiescent (1970–1992) periods. Units are knots [1 knot (kt) = 0.51 m s^{-1}] per 6-hr. Data are provided in bins of 5 kt resolution. Error bars show ±σ (s.d.) from the mean probability density for that bin (based on bootstrap sampling). Actual counts of 6-hr intensification rates for hurricanes (**c**) and major hurricanes (**d**). Empirical cumulative distribution functions of hurricane (**e**) and major hurricane (**f**) intensification rates and their 95% confidence bounds (dashed lines). All data are taken from the region denoted by the northernmost white-outlined region in Fig. 2a, and only intensification rates over water are included, i.e., weakening due to landfall does not contribute.

Figure 4 | Pattern of Atlantic SST trends. SST trend pattern over the period 1948–2015 in units of standard deviation per decade. Hatching shows regions where the trends are *not* significant.

Figure 1:

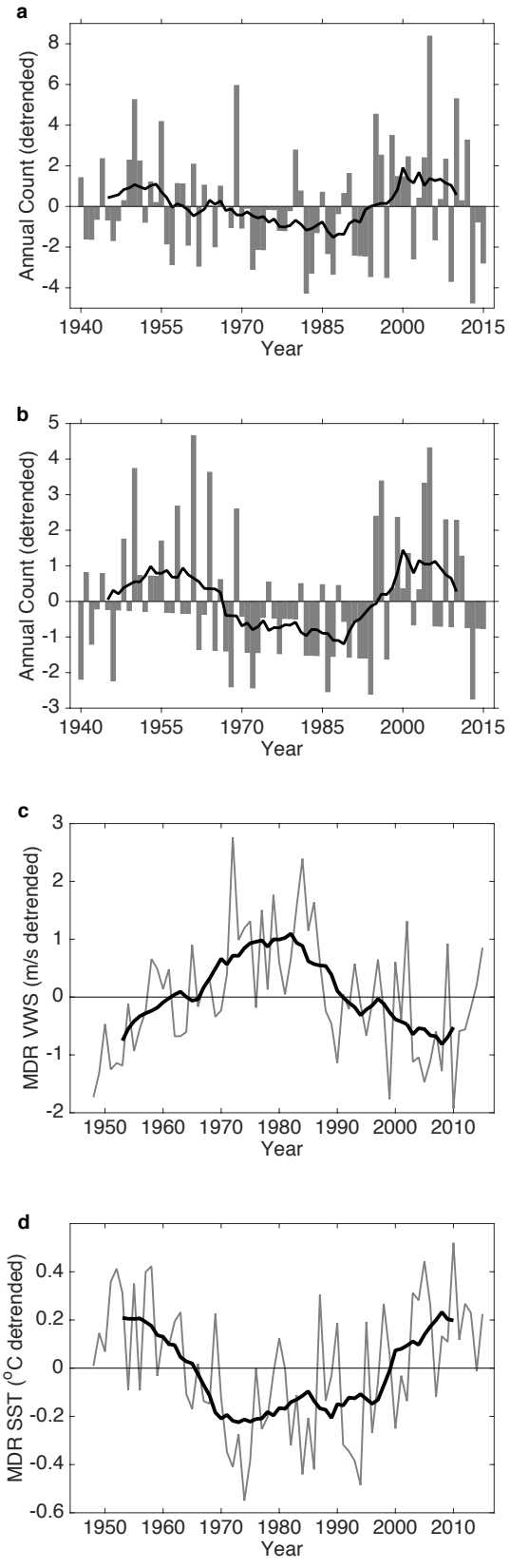
a
Annual Count (detrended)
8
6
4
2
0
-2
-4
1940
1955
1970
1985
2000
2015
Year
b
Annual Count (detrended)
5
4
3
2
1
0
-1
-2
-3
1940
1955
1970
1985
2000
2015
Year
c
MDR VWS (m/s detrended)
3
2
1
0
-1
-2
1950
1960
1970
1980
1990
2000
2010
Year
d
MDR SST (°C detrended)
0.4
0.2
0
-0.2
-0.4
-0.6
1950
1960
1970
1980
1990
2000
2010
Year

Figure 2:

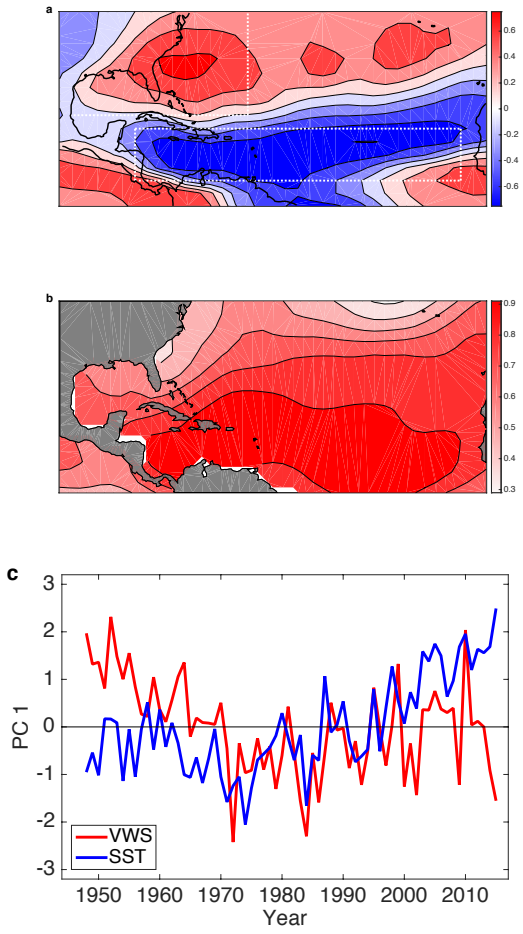
a
0.6
0.4
0.2
0
-0.2
-0.4
-0.6
b
0.9
0.8
0.7
0.6
0.5
0.4
0.3
c
PC 1
3
2
1
0
-1
-2
-3
VWS
SST
1950
1960
1970
1980
1990
2000
2010
Year

Figure 3:

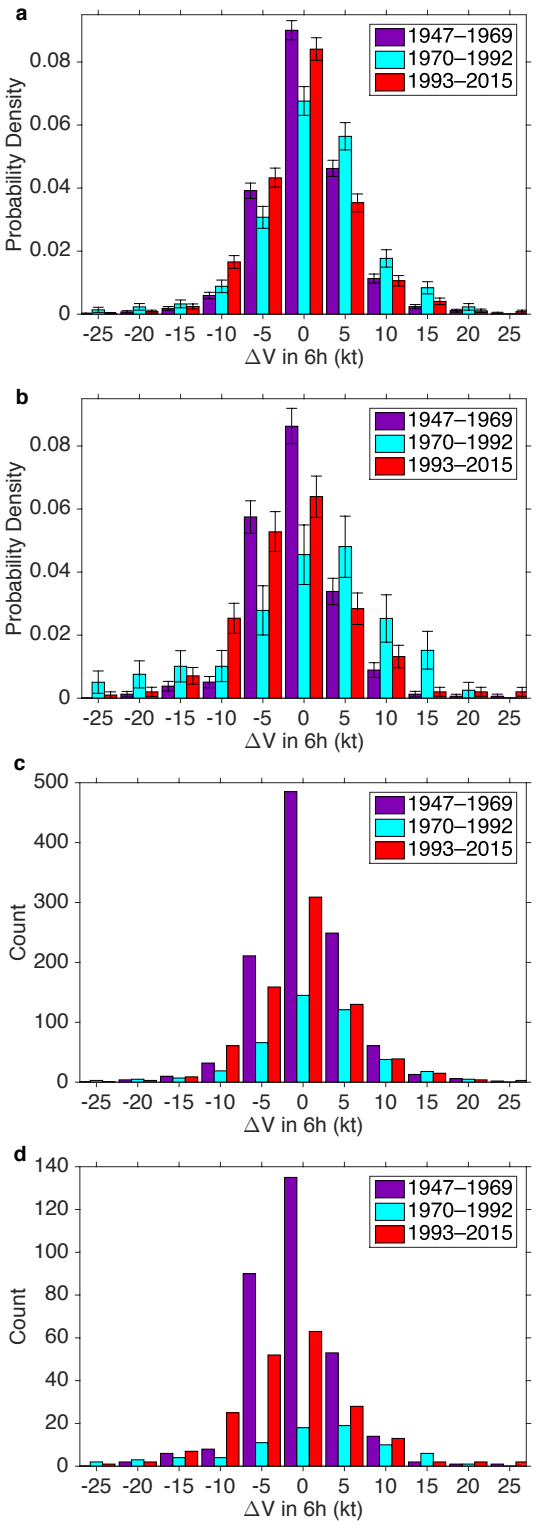
a
b
c
d
1947–1969
1970–1992
1993–2015
Probability Density
Count
ΔV in 6h (kt)

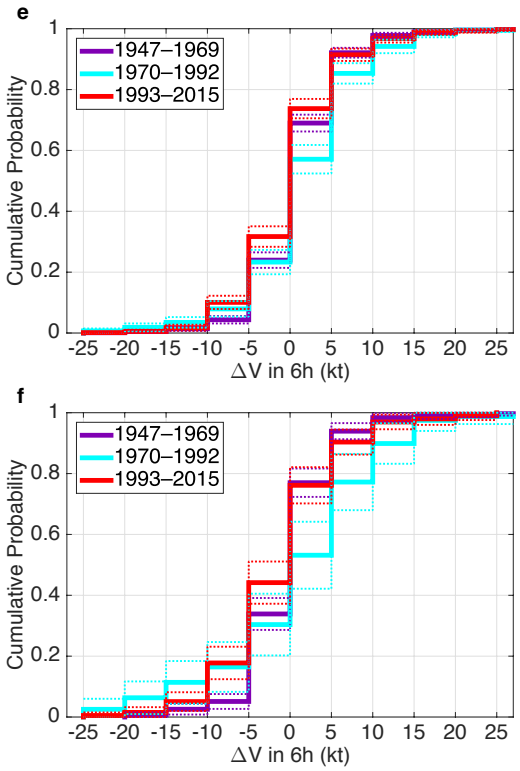
e
1947–1969
1970–1992
1993–2015
Cumulative Probability
ΔV in 6h (kt)
f
1947–1969
1970–1992
1993–2015
Cumulative Probability
ΔV in 6h (kt)

Figure 4: